Earth Syst. Dynam. Discuss., 2, 393–434, 2011
www.earth-syst-dynam-discuss.net/2/393/2011/
doi:10.5194/esdd-2-393-2011

Earth System Dynamics Discussions

MEP solution for a minimal climate model: success and limitation of a variational problem

S. Pascale[1], **J. M. Gregory**[1,4,2], **M. H. P. Ambaum**[1], **R. Tailleux**[1], **and V. Lucarini**[1,3]

[1]Department of Meteorology, University of Reading, UK
[2]Met Office Hadley Centre, Exeter, UK
[3]Department of Mathematics, University of Reading, UK
[4]NCAS-Climate, University of Reading, UK

Received: 17 May 2011 – Accepted: 18 May 2011 – Published: 23 May 2011

Correspondence to: Salvatore Pascale (s.pascale@reading.ac.uk)

Published by Copernicus Publications on behalf of the European Geosciences Union.

Abstract

Maximum Entropy Production conjecture (MEP) is applied to a *minimal* four-box model of climate which accounts for both horizontal and vertical material heat fluxes. It is shown that, under condition of fixed insolation, a MEP solution is found with reasonably realistic temperature and heat fluxes, thus generalising results from independent two-box horizontal or vertical models. It is also shown that the meridional and the vertical entropy production terms are independently involved in the maximisation and thus MEP can be applied to each subsystem with fixed boundary conditions. We then extend the four-box model by increasing its number of degrees of freedom, and test its realism by comparing it with a GCM output. An order-of-magnitude evaluation of contributions to the material entropy production ($\approx$50 mW m^{-2} K^{-1}) due to horizontal and vertical processes within the climate system is carried out by using *ad hoc* temperature fields. It turns out that approximately 40 mW m^{-2} K^{-1} is the entropy production due to vertical heat transport and 5–7 mW m^{-2} K^{-1} to horizontal heat transport. A MEP solution is found which is fairly realistic as far as the horizontal large scale organisation of the surface climate is concerned whereas the vertical structure looks to be unrealistic and presents seriously unstable features. Finally a more general problem is investigated in which the longwave transmissivity is varied simultaneously with the temperature. This leads to a MEP solution characterised by a much warmer climate, with very vigorous vertical heat fluxes, in which the atmosphere is opaque to longwave radiation. A critical discussion about how to interpret MEP and how to apply it in a physically correct way concludes the paper.

1 Introduction

Since Paltridge's seminal paper (Paltridge, 1975) it has been debated whether the meridional structure of the climate can be explained by the Maximum Entropy Production conjecture (MEP). Such a hypothesis, often controversial (Goody, 2007; Caldeira,

ESDD
2, 393–434, 2011

2007), has been mainly tested through simple energy-balance box-models (Paltridge, 1975, 1978, 1981; Grassl, 1981; Lorenz et al., 2001; Kleidon, 2004; Jupp and Cox, 2010; Kleidon, 2010; Herbert et al., 2010). Such relatively simple box-models have become the paradigm to demonstrate MEP and used also to explain the vertical structure of the atmosphere (Kleidon, 2009). In such models MEP is understandable very simply as a trade-off between the heat flux and the temperature difference (the thermodynamical force) which drives the flux: steady states with very high meridional temperature contrasts are consistent with low meridional heat transport and steady states with very low temperature contrasts with high energy transports. For both of them the entropy production tends to zero as either the heat flux or the temperature difference goes to zero. There is therefore a "trade-off" between heat transport and temperature contrast whereby entropy production is maximised in some intermediate state. Whether the climate really is in a MEP state remains however still to be demonstrated despite some evidence which has built up in geosciences and despite its attraction of offering a beautiful unifying picture for all disequilibrium processes in the Earth system (Kleidon, 2010). An *ab initio* rigorous proof however is still missing (Dewar, 2005; Grinstein and Linsker, 2007) as well as a more general theoretical framework, consistent either with non-equilibrium Statistical Mechanics or fundamental thermodynamics, into which MEP may fit and which may unify the several co-related extremal principles known in Fluid Dynamics.

The total material entropy production of the climate system has been estimated to be about 50 $\mathrm{mW\,K^{-1}\,m^{-2}}$ and most of it is associated with the hydrological cycle (Fraedrich and Lunkeit, 2008; Pascale et al., 2011a). Entropy production associated with meridional heat transport represents ($\leq$10 $\mathrm{mW\,K^{-1}\,m^{-2}}$) a small fraction of the overall material entropy production and therefore box-model MEP proofs which consider only the horizontal dimension are incomplete. To the authors' knowledge the only studies of MEP taking account of both horizontal and vertical material entropy production are the ones in Noda and Tokioka (1983) and Herbert et al. (2011). Noda and Tokioka (1983) extended Paltridge's work to a two-dimensional zonal model with prescribed

ESDD
2, 393–434, 2011

water vapour but variable low, middle and high clouds. However the MEP solutions they found were shown to be very sensitive to the parametrisation of humidity, since either multiple maxima or no maximum at all could be obtained for certain distribution of relative humidity. Herbert et al. (2011) presented a new formulation of Paltridge's model in which the *Net-Exchange Formulation* of radiative transfer is employed (Dufresne et al., 2005), the *ad hoc* convective hypothesis of Paltridge (1978) is avoided and the total material entropy production maximised, but they do not account for the vertical resolution of the atmosphere.

In this paper we will apply MEP to a very simple two-dimensional zonal-vertical climate model able to account for the total material entropy production due to both horizontal and vertical heat fluxes. Firstly a simple minimal four-box model will be used to study the MEP solution and understand the relations between horizontal and vertical entropy production in the maximisation process (Sect. 2). Secondly we we will extend the number of degrees of freedom of the model (Sect. 3) in order to compare our results with more realistic GCM studies of the climatic entropy budget (Pascale et al., 2011a), to give an estimate of the decomposition of the total material entropy production into its horizontal and vertical component (Sect. 4) and to account for the vertical resolution of the atmosphere. A MEP solution will be found by keeping the optical atmospheric properties fixed and varying only the temperature (Sect. 5), keeping the longwave transmissitivities at realistic climatological values. In Sect. 6 we relax the physical constraints and a problem in which not only the temperature field but also the longwave transmittivities are varied. The new MEP solution turns out to be unrealistic. In the final section (Sect. 7) we discuss findings in Sect. 5 and Sect. 6 in relation to the new results from Pascale et al. (2011b), criticism from Goody (2007) and recently proposed points of view of MEP (Dewar, 2009; Dyke and Kleidon, 2010).

ESDD
2, 393–434, 2011

2 Minimal box-model for material entropy production

2.1 The model

A minimal conceptual box-model for climatic entropy production is shown in Fig. 1, where by 1 we denote the tropical zone and by 2 the extratropical one. The atmospheric boxes have longwave and shortwave transmittivities, $\tau_{l,i}$, $\tau_{s,i}$, $i = 1,2$ (see Table 1), the longwave emissivity is assumed to be $\epsilon_i = 1 - \tau_{l,i}$ and the surface interacts with the atmosphere through the vertical fluxes of latent and sensible heat, H_1 and H_2. Atmospheric boxes also exchange energy due to the meridional heat flux M. Assuming the system to be in a steady state, we have for each box:

$$I_1(1-\tau_{s,1}) + H_1 - M + (1-\tau_{l,1})(G_1 - 2A_1) = 0, \quad (1)$$

$$I_2(1-\tau_{s,2}) + H_2 + M + (1-\tau_{l,2})(G_2 - 2A_2) = 0, \quad (2)$$

$$\tau_{s,1}I_1 - G_1 - H_1 + (1-\tau_{l,1})A_1 = 0, \quad (3)$$

$$\tau_{s,2}I_2 - G_2 - H_2 + (1-\tau_{l,2})A_2 = 0, \quad (4)$$

where $G_i = \sigma T_{g,i}^4$ and $A_i = \sigma T_{a,i}^4$ and σ is the Stefan-Boltzmann constant. Such a model has no albedo-, cloud-, and water vapor- feedback since the albedo and the transmittivities are fixed. As a consequence the net insolation of each box, I_1, I_2, which in general depends on surface and atmosphere state (surface and planetary albedo), is fixed as well. From Eqs. (1–4) after some algebra we have:

$$\sigma T_{a1}^4 = \frac{I_1(1-\tau_{l,1}\tau_{s,1}) + \tau_{l,1}H_1 - M}{1-\tau_{l,1}^2}, \quad (5)$$

$$\sigma T_{a2}^4 = \frac{I_2(1-\tau_{l,2}\tau_{s,2}) + \tau_{l,2}H_2 + M}{1-\tau_{l,2}^2}, \quad (6)$$

$$\sigma T_{g1}^4 = \frac{(1+\tau_{s,1})I_1 - H_1 - M}{1+\tau_{l,1}}, \quad (7)$$

ESDD
2, 393–434, 2011

$$\sigma T_{g2}^4 = \frac{(1+\tau_{s,2})I_2 - H_2 + M}{1+\tau_{l,2}} \tag{8}$$

and by considering the temperatures as functions of M, H_1, H_2, we have a whole set of steady states, each specified by values of three heat exchanges M, H_1, H_2.

The material entropy production in the box-model shown in Fig. 1 is generated by three different fluxes M, H_1 and H_2 which carry heat through the temperature differences $T_{a,1} - T_{a,2}$, $T_{g,1} - T_{a,1}$, $T_{g,2} - T_{a,2}$ (i.e. by the fluid response to the radiative forcing) and it reads:

$$\dot{S}_{\mathrm{mat}} = M\left(\frac{1}{T_{a2}} - \frac{1}{T_{a1}}\right) + H_1\left(\frac{1}{T_{a1}} - \frac{1}{T_{g1}}\right) + H_2\left(\frac{1}{T_{a2}} - \frac{1}{T_{g2}}\right). \tag{9}$$

$\dot{S}_{\mathrm{mat}}$ is therefore the sum of two different contributions: $\dot{S}_{\mathrm{mer}} = M(1/T_{a,1} - 1/T_{a,2})$ due to the horizontal motions of the atmosphere and $\dot{S}_{\mathrm{ver}} = H_1(1/T_{a,1} - 1/T_{g,1}) + H_2(1/T_{a,2} - 1/T_{g,2})$ due to surface-atmosphere coupling through convective fluxes. In the real climate $\dot{S}_{\mathrm{ver}}$ can be thought as the entropy production due to the hydrological cycle (latent heat) and to sensible heat fluxes at the surface (Kleidon, 2009). Lucarini et al. (2010) have shown that $\dot{S}_{\mathrm{mer}}$ is approximately a lower bound of entropy production due to dissipation of kinetic energy. Material entropy production is a function of (M, H_1, H_2) and thus defined in the (M, H_1, H_2) space. Material entropy production terms $\dot{S}_{\mathrm{mer}}$, $\dot{S}_{\mathrm{ver},1}$ and $\dot{S}_{\mathrm{ver},2}$ have to be positive in order not to violate the second law of thermodynamics, i.e. $\dot{S}_{\mathrm{mer}} \geq 0$, $\dot{S}_{\mathrm{ver1}} \geq 0$, $\dot{S}_{\mathrm{ver2}} \geq 0$ simultaneously. Such constraints limit further the acceptable values (M, H_1, H_2), as shown in Figs. 2–5.

2.2 MEP solution

$\dot{S}_{\mathrm{mat}}$, shown in Figs. 2a–3a, has a unique maximum for $(M_{\mathrm{mep}}, H_{1,\mathrm{mep}}, H_{2,\mathrm{mep}}) \approx (34.5, 113, 55)\,\mathrm{W\,m^{-2}}$ inside the physical region (shown on the graphs). Values of energy fluxes, temperatures and entropy production of the MEP solution are summarised

ESDD
2, 393–434, 2011

in Table 2 and compared with HadCM3 climatology, revealing a certain degree of realism particulalry in the atmospheric temperatures and heat fluxes. Surface temperatures are generally lower than HadCM3 climatology and also the material entropy production is generally underestimated by the MEP solution.

From Fig. 3b we observe that the horizontal component of the material entropy production $\dot{S}_{\mathrm{mer}}$ is quasi-independent from H_1 and H_2, in that the highest values are placed at $M \approx 30\ \mathrm{W\,m^{-2}} \approx M_{\mathrm{mep}}$ regardless of H_1 (and H_2, not shown). As for $\dot{S}_{\mathrm{mer}}$, the value of $\dot{S}_{\mathrm{ver},1}$ ($\dot{S}_{\mathrm{ver},2}$) is maximised by the same H_1 (H_2) regardless of M. There is therefore a kind of "orthogonality" in the material entropy production which allows us to formulate the MEP conjecture for either $\dot{S}_{\mathrm{mer}}$ or $\dot{S}_{\mathrm{ver}}$ separately. Therefore, for example, a climate could be in a state of maximum horizontal entropy production without maximising the total material entropy production. $\dot{S}_{\mathrm{ver}}$ (Fig. 5a–b) has a very weak dependence on the meridional heat transport M (Fig. 5a) and shows a well defined peak only in the (H_1, H_2) plane for $M = M_{\mathrm{MEP}}$, but not a unique maximum as $\dot{S}_{\mathrm{mat}}$. This is consistent with the approximation of the climate as a vertical surface-atmosphere system, as the one considered in Kleidon (2009) under MEP requirements.

The main difference between $\dot{S}_{\mathrm{mat}}$ and $\dot{S}_{\mathrm{mer}}, \dot{S}_{\mathrm{ver},1}, \dot{S}_{\mathrm{ver},2}$ is that only the first one has a unique local maximum whereas the last three exhibit a sort of ridge but no local maxima, on account of the orthogonality, at least in the physical range for the parameters. Therefore from this model we learn that MEP can uniquely predict the overall flux structure of this climate model only when the whole material entropy production is taken into account. However the same plots show that if we restrict ourselves to either the atmosphere or the vertical subsystem surface-atmosphere of our model, and regard the other fluxes external to these as fixed boundary conditions, we retrieve MEP for that particular subsystem. As far as the vertical atmosphere is concerned, studies with more realistic continuous vertical models come from Pujol and Fort (2002) and Ozawa and Ohmura (1997) but without any consideration of horizontal fluxes.

ESDD
2, 393–434, 2011

3 Generalization of the minimal box-model

3.1 Experiment setup and material entropy production

Let us consider a generalisation of the climate model shown in Fig. 1. We maintain the same physics but increase the spatial resolution. The interior of the ocean is neglected since the material entropy production due to the small-scale eddy turbulence ($\sim$1 mW m^{-2} K^{-1}) is negligible when compared to the material entropy production of the whole climate system ($\sim$50 mW m^{-2} K^{-1}, see Pascale et al., 2011a). The solar energy input (shortwave heating rates within the atmosphere, shortwave fluxes at the surface and top of the atmosphere) is fixed and taken from a 30-year mean FAMOUS control run (Smith et al., 2008). This ensures fixed "forcing" boundary conditions in full analogy with the minimal 4-box model considered in Sect. 2.1. Fixing the solar input is a very restrictive assumption since in the real climate the shortwave cloud feedback and the sea-ice feedback are very important state-dependent mechanisms which can substantially alter the amount of solar heating received by climate components, but this is a simplifying hypothesis often assumed in the MEP literature (Lorenz et al., 2001; Rodgers, 1976; Murakami and Kitoh, 2005; Ozawa and Ohmura, 1997; Pujol and Fort, 2002; Kleidon et al., 2003, 2006; Kunz et al., 2008).

As mentioned above, we will use the FAMOUS model for working out the solar forcing and, in the following, longwave properties to be used in our box-model. FAMOUS (FAst Met Office/UK Universities Simulator) is the low resolution version of HadCM3 (Gordon et al., 2000; Pope et al., 2000), which has been widely used to simulate present day and future climate. The atmosphere model of FAMOUS has a horizontal grid spacing of $5^\circ \times 7.5^\circ$ and 11 vertical levels whereas HadCM3 $2.5^\circ \times 3.75^\circ$ and 19 vertical levels. FAMOUS and HadCM3 solutions can be considered a relatively good representation of real climatology, as shown in Jones et al. (2005). Therefore in the following we will use them to compare MEP solutions.

Also we note that climate steady state emerges from time-dependent forcing by the diurnal and seasonal cycle, whereas here, as in almost all MEP literature, we define

ESDD
2, 393–434, 2011

the MEP model with time-independent boundary conditions. Although the seasonal and diurnal cycle imply small variations compared with the annual mean, because of non-linearity of the system the time-dependent forcing could plausibly affect the time-mean state. This is an issue which deserves further investigation.

The longwave optical properties of the atmosphere (emissivity, transmissivity, scattering) are in general very complex functions of the concentrations of the absorbing gases and aerosols and of the climatic state (pressure, temperature, cloud cover). A fully consistent treatment would thus demand a state-of-the-art radiative scheme. In order to keep the simplicity of the model discussed in Sect. 2 we make here the drastic assumption of constant emissivity and transmissivity in each grid-box. Furthermore, we neglect the scattering of longwave radiation (which however is accounted for in FAMOUS). This is justified by the high asymmetry factors and the low single scattering albedo for infrared radiation (Edwards and Slingo, 1996), which make effects of absorption dominant compared with those of scattering. The main effect of longwave radiation scattering is a reduction of the OLR of $\sim 2\,\mathrm{W\,m^{-2}}$ Edwards and Slingo (1996).

We deduce the broad mean transmissivity of each atmospheric layer from a FAMOUS mean state for which the upwelling and downwelling longwave fluxes are available at each model half level (interfaces between model layers), say $L_{z+1/2}(\uparrow), L_{z+1/2}(\downarrow)$. By assuming that each grid-box of mean transmissivity τ emits e upwards and downwards, we must have that

$$L_{z+1/2}(\uparrow) = e_z + \tau_z L_{z-1/2}(\uparrow), \tag{10}$$

$$L_{z-1/2}(\downarrow) = e_z + \tau_z L_{z+1/2}(\downarrow), \tag{11}$$

from which the following estimate for τ_z at every model level z are obtained:

$$\tau_z = \frac{L_{z+1/2}(\uparrow) - L_{z-1/2}(\downarrow)}{L_{z-1/2}(\uparrow) - L_{z+1/2}(\downarrow)}, \tag{12}$$

We define the emissivity at each grid-point either as $\epsilon \equiv e/\sigma T_a^4$, by using the energy emissions found in Eq. (10), or as $\epsilon = 1 - \tau$, in full analogy with the model in Sect. 2.1.

ESDD
2, 393–434, 2011

The definitions of ϵ do not exactly coincide (differences of percents) as we would expect given the very crude approximation implied by Eqs. (10)–(11) in which we neglect to account for the longwave scattering and spectral dependance (as it is in Edwards and Slingo (1996)). The first definition allows us to match the model entropy budget and the TOA fluxes and therefore should be seen more like a parametrisation of the box model against climatology.

3.2 Radiative heating rates and entropy production

Given the longwave transmittivities $\tau(\mathbf{x})$ and emissivities $\epsilon(\mathbf{x})$, the longwave heating rates $Q_{lw}(\mathbf{x})$ can be obtained at every grid-point as a function of the temperature field. From Eq. (11) we have that for N, the top atmospheric layer, $L_{N-1/2}(\downarrow) = \epsilon_N \sigma T_{a,N}^4$ since the downwelling longwave fluxes are null at the TOA (half level $N+1/2$). Hence by iteration all the downwelling longwave fluxes can be obtained for any temperature profile within the column. Likewise a similar iterative process is applied to obtain the upwelling fluxes $L(\uparrow)$ by using equation in Eq. (10) once the lowest value is set $L_{1/2}(\uparrow) = \sigma T_g^4$. The knowledge of both upwelling and downwelling longwave fluxes for any given temperature field allows the calculation of the longwave heating rates as $Q_{\text{lw}} = -\partial_z(L(\uparrow) + L(\downarrow))$ and hence

$$Q_{\text{lw}} = Q_{\text{lw}}[T(\mathbf{x})]. \tag{13}$$

Adding the prescribed shortwave heating to Q_{lw}, we obtain the net radiative heating:

$$Q_{\text{rad}}[T(\mathbf{x})] = Q_{\text{sw}}(\mathbf{x}) + Q_{\text{lw}}[T(\mathbf{x})]. \tag{14}$$

As shown in Goody (2000) and Pascale et al. (2011a) the material entropy production can be expressed in terms of the radiative heating rates:

$$\dot{S}_{\text{mat}} = -\int \frac{Q_{\text{rad}}}{T} dV \tag{15}$$

ESDD
2, 393–434, 2011

where the integral is over the climate system and T denotes T_a inside the atmosphere and T_s at the surface. Therefore from Eqs. (13), (14) and (15) it is seen that the material entropy production is defined as a positive-definite functional of the climate temperature field, i.e. $\dot{S}_{\mathrm{mat}} = \dot{S}_{\mathrm{mat}}[T(\mathbf{x})]$. The only constraint we have to maintain on the temperature field is:

$$\int_{CS} Q_{\mathrm{rad}}[T(\mathbf{x})]dV = 0, \tag{16}$$

which is required to ensure a steady state. Using $T(\mathbf{x})$ from FAMOUS, the value of the material entropy production we estimate is about $47\,\mathrm{mW\,m^{-2}\,K^{-1}}$, that is around $5\,\mathrm{mW\,m^{-2}\,K^{-1}}$ less than the value diagnosed from FAMOUS in Pascale et al. (2011a). This is due to the the fact that here we use time means $\overline{(\cdot)}$ for calculations and at the surface $\int \overline{Q_{\mathrm{sw}}}/\overline{T_s} - \overline{\int Q_{\mathrm{sw}}/T_s} \sim 5\,\mathrm{mW\,m^{-2}\,K^{-1}}$.

4 Vertical and horizontal entropy production

Before considering MEP, let us examine some special significant temperature fields under the energy requirement Eq. (16), in order to estimate the *horizontal* component $\dot{S}^{\mathrm{mer}}_{\mathrm{mat}}$ and the *vertical* component $\dot{S}^{\mathrm{ver}}_{\mathrm{mat}}$ of the material entropy production. However, because of the very drastic simplification assumed in the model formulation (e.g. fixed prescribed longwave optical properties), such temperature fields will not be fully consistent with the prescribed shortwave and longwave absorptions which in reality generally depend on temperature 1. Therefore we will take them more as an order-of-magnitude estimate rather than precise ones.

4.1 Null entropy production

The first two temperature fields we look at are the "constant temperature" solution $T_{\mathrm{NOT}} \sim 250\,\mathrm{K}$ (NOT stands for NO Temperature gradient) for both surface and

ESDD
2, 393–434, 2011

atmosphere and the radiative solution T_{NOH}, which is characterised by the fact that the radiative heating in each grid-box is zero and therefore no convergence of "material" heat fluxes is required (NOH, that is NO Heat). T_{NOH} is found with the help of the IDL subroutine IMSL_ZEROSYS by solving, for each vertical column, a set of $N+1$ (surface+atmospheric levels) non-linear equations:

$$Q_{\mathrm{lw},z}[T_s, T_1, \ldots, T_N] + Q_{\mathrm{sw},z} = 0, \quad z = 1, \ldots, N+1. \tag{17}$$

A reduction of the degrees of freedom of the fields is necessary in order to obtain a numerical solution with the IDL routine. We reduce the degrees of freedom by taking the zonal mean of the fields and interpolating in latitude from 37 (FAMOUS) to 17 points. This reduce the degrees of freedom of a factor 200 and makes the numerical problem more tractable.

Both cases are characterised by null material entropy production, since the radiative solution corresponds to a climate without any heat transport whereas the constant solution is the one in which the heat is transported around sufficiently vigorously by as to smooth out any temperature gradient. The main differences between these two climates and the FAMOUS climate can be seen in Fig. 8a–b. NOH has neither meridional heat transport nor vertical heat transport but very strong meridional and vertical temperature contrasts (including a large near-surface step). This is because material heat transport in reality mitigates the latitudinal contrast of insolation, and reduces the instability of the vertical temperature profile. The NOT climate has very large meridional and vertical heat transports, much larger than in FAMOUS, required to erase all the radiatively imposed temperature contrasts.

4.2 Vertical entropy production

In order to have states with no horizontal entropy production $\dot{S}^{\mathrm{mer}}_{\mathrm{mat}} \approx 0$ and thus solely vertical entropy production $\dot{S}_{\mathrm{mat}} \approx \dot{S}^{\mathrm{ver}}_{\mathrm{mat}}$, there are two possibilities: to suppress either meridional temperature gradients or the meridional heat flux. We call NOHT (NO Horizontal Temperature gradient) the case associated with a temperature field T_{NOHT} which

ESDD
2, 393–434, 2011

is horizontally homogeneous, i.e. with no meridional temperature gradients, but which still preserves a vertical structure. Such a field is obtained by replacing the actual temperatures with their model level means. Let us note (Fig. 8a) that the meridional heat transport in NOHT is larger than the one in NOT, where also the vertical temperature gradient has been suppressed. Secondly we consider a temperature field T_{NOHH} which has the characteristic of producing a TOA longwave radiation equal to the net incoming shortwave one. This is obtained if $T_{\mathrm{NOHH}} = T_{\mathrm{CLIM}}(\alpha)^{1/4}$, where α is the ratio between the magnitude of the net shortwave and longwave fluxes at the top of the atmosphere followed by a small adjustment in order to satisfy Eq. (16). Consequently such climate (NOHH, NO Horizontal Heat) has no meridional heat transport (Fig. 8a).

By using our approximation we find $\dot{S}_{\mathrm{mat}} \approx 39\,\mathrm{mW\,m^{-2}\,K^{-1}}$ and $\dot{S}_{\mathrm{mat}} \approx 41\,\mathrm{mW\,m^{-2}\,K^{-1}}$ for T_{NOHT} and T_{NOHH} respectively. Other estimates obtained from vertical radiative-convective models in MEP states, though under different modelling assumptions, are: $24\,\mathrm{mW\,m^{-2}\,K^{-1}}$ (Kleidon, 2009, two-box model), $21.3\,\mathrm{mW\,m^{-2}\,K^{-1}}$ (our four-box model of Table 2), $54\,\mathrm{mW\,m^{-2}\,K^{-1}}$ (Ozawa and Ohmura, 1997, vertical continuous model), $56\,\mathrm{mW\,m^{-2}\,K^{-1}}$ (Pujol and Fort, 2002, vertical continuous model), $40\,\mathrm{mW\,m^{-2}\,K^{-1}}$ (Wang et al., 2008, vertical continuous model with clouds). The reason for these difference is due to the structural diversity of the models employed to study MEP.

4.3 Horizontal entropy production

Finally let us consider a temperature field T_{NOVT} which is vertically homogeneous (NOVT, NO Vertical Temperature gradient): the temperature is constant throughout each vertical column ($\partial_z T = 0$, including the surface as well) but with a meridional gradient. Such a field is obtained by replacing the actual field with the its vertical weighted average plus a small adjustment in order to satisfy Eq. (16). As a consequence $\dot{S}^{\mathrm{ver}}_{\mathrm{mat}} \approx 0$ and hence $\dot{S}_{\mathrm{mat}} \approx \dot{S}^{\mathrm{mer}}_{\mathrm{mat}}$. We find that $\dot{S}_{\mathrm{mat}} \approx 6\,\mathrm{mW\,m^{-2}\,K^{-1}}$, which is almost complementary to the values found for T_{NOHT} and T_{NOHH} ($\approx 40\,\mathrm{mW\,m^{-2}\,K^{-1}}$) with respect to the overall material entropy production ($\sim 47\,\mathrm{mW\,m^{-2}\,K^{-1}}$) refer back to

ESDD
2, 393–434, 2011

the earlier finding of orthogonality in the 4-box model. It is similar to estimates of the entropy production due to meridional heat transport found in one-dimensional horizontal models (7 mW m^{-2} K^{-1} (Kleidon, 2009), 8.8 mW m^{-2} K^{-1} (Paltridge, 1978)). We are led to conclude that most of the material entropy production 85 %) can be thought of as associated with vertical heat transport and the remaining (∼15 %) with horizontal heat transport.

5 The variational problem and MEP solution

The Maximum Entropy Production conjecture applied to the model presented in this chapter can be formulated as a constrained variational problem (Noda and Tokioka, 1983; Schulman, 1977; Ito and Kleidon, 2005): the MEP temperature field is the one which maximises $\dot{S}_{\mathrm{mat}}$ under the energy balance constraint Eq. (16). For our model such a solution is defined as the field T_{MEP} such that:

$$\frac{\delta \dot{S}_{\mathrm{mat}}}{\delta T}[T_{\mathrm{MEP}}] = 0 \quad \text{and} \quad \int_{CS} Q_{\mathrm{rad}}[T_{\mathrm{MEP}}]dV = 0, \tag{18}$$

where δ is the functional derivative. We have assumed no surface net heat flux into the ocean and therefore radiative fluxes and latent-sensible heat fluxes balance each other at the surface. A numerical solution is found by using the IDL optimisation routine IMSL_CONSTRAINED_NLP, which allows to deal with maximisation problems under non-linear constraints (Spellucci, 1998). Again we need to reduce the degrees of freedom, as explained in Sect. 4.1, in order to make the problem affordable for the IDL numerical routine. Two numerical solutions, T_{MEP} and T_{MEP2}, are found for the $\epsilon = e/\sigma T^4$ and $\epsilon = 1 - \tau$ case (Figs. 7a and 9b), which in the following we will refer as MEP and MEP2 respectively. IMSL_CONSTRAINED_NLP accepts an optional initial guess from which the numerical search is started. Different initial guesses (T_{CLIM}, T_{NOHT}, T_{NOVT}) are then used with IMSL_CONSTRAINED_NLP in order to test the convergence of the numerical solution and exclude the possibility of multiple maxima.

ESDD
2, 393–434, 2011

5.1 Comparison with the model solution

The MEP and MEP2 solutions are compared with the FAMOUS climatology in Fig. 7b and they turn out to be fairly similar between them. The value of the material entropy production for MEP is $\dot{S}_{\mathrm{mat}}[T_{\mathrm{MEP}}] \sim 70\,\mathrm{mW\,m^{-2}\,K^{-1}}$, which is larger than the FAMOUS one (about $50\,\mathrm{mW\,m^{-2}\,K^{-1}}$) and than any other value obtained from the different temperature fields examined in Sect. 4 (see Table 3). MEP2 is instead associated to an entropy production $\approx 57\,\mathrm{mW\,m^{-2}\,K^{-1}}$. The MEP and MEP2 fields related to the horizontal structure (i.e. surface temperature, atmospheric temperature, meridional heat transport) are fairly close to FAMOUS solution. This is true for the surface temperature field (Figs. 8a and 10a) and the meridional heat transport (Figs. 8b and 10b).

The MEP (MEP2) solution looks to be intermediate between NOHT and NOHH which have, respectively, the largest and the smallest meridional heat transport and, conversely, the smallest and the largest equator-to-pole temperature difference (Fig. 8a). Also when we consider NOVT we see that the vertical material heat flux of the MEP solution is intermediate between NOVT and the case with no vertical heat flux. Therefore, as already discussed in Kleidon (2009), a trade-off between fluxes and temperature differences seems to justify the maximum in the material entropy production.

The main differences between the MEP (MEP2) solution and the FAMOUS one are in the vertical structure. It can be seen that T_{MEP} and T_{MEP} tend to be warmer than T_{CLIM} in the upper atmosphere and colder in the lower atmosphere. This feature is clearly seen in the global mean of the temperature profiles in Figs. 8b and 10c. The MEP (MEP2) solution is more vertically mixed and reasonably in agreement with the one shown at page 443 of Ozawa and Ohmura (1997). The second remarkable difference is the discontinuity between surface temperature and near-surface atmospheric temperature, which in the MEP (MEP2) solution is unrealistically large ($\approx$6 K whereas in FAMOUS it is < 1 K). The MEP solution shows this feature also in Pujol and Fort (2002), who found a difference between the ground temperature and the air temperature at the surface ~ 10 K. Of course the model (and the real climate) cannot have such a temperature discontinuity, which turns out to be convectively unstable.

ESDD
2, 393–434, 2011

The MEP and MEP2 solutions have a mean surface vertical heat flux of nearly $80\,\mathrm{W\,m^{-2}}$ (Fig. 10d), which is lower than the FAMOUS one ($\approx 100\,\mathrm{W\,m^{-2}}$), and it is also lower in the two first atmosphere levels. Such a low value, which is in very good agreement with the one found by Pujol and Fort (2002) in their one dimensional model, explains the large discontinuity of the temperature at the surface. In the middle- and upper- atmosphere the mean vertical heat flux exceeds the one of the the FAMOUS solution. This means that a larger amount of heat is carried upwards which reduces the mean lapse rate and thus increases the atmospheric stability. The differences in the vertical structure is therefore the key element for explaining the difference in entropy production between the FAMOUS and the MEP (MEP2) solution.

It is questionable whether such a solution is general enough for debating MEP validity, since the longwave transmissivity τ (Sect. 3.1) is prescribed and the temperature varied, whereas τ should be varied as well consistently with T_a. Nevertheless we may say that if the actual model solution is one of maximum entropy production, this should coincide with the one found here, which does not appear to be the case.

5.2 Vertical contributions to $\dot{S}_{\mathrm{ver}}$

In order to gain some qualitative understanding about the magnitude of the entropy produced by vertical heat transport we reduce the two-dimensional configurations to vertical one-dimensional ones. This is obtained by averaging over the horizontal levels in order to eliminate the convergence of meridional heat transport. For an energy-balance model (no dynamics), given radiative, vertical and horizontal material heat fluxes **R**, **H**, **M**, in a steady state we must have:

$$\nabla\cdot\mathbf{R}+\nabla\cdot\mathbf{H}+\nabla\cdot\mathbf{M}=0. \tag{19}$$

By defining the area-average as $\overline{(\cdot)}\equiv\int_\Sigma(\cdot)d\sigma/\int_\Sigma d\sigma$ and integrating over the k-th horizontal model level, of area Σ_k, we get rid of **M**:

$$\int_{\Sigma_k} Q_{\mathrm{rad},k}\,d\sigma+\int_{\Sigma_k}\nabla\cdot\mathbf{H}\,d\sigma=0 \tag{20}$$

ESDD
2, 393–434, 2011

because $\int_\Sigma \nabla\cdot\mathbf{M}\,d\sigma = 0$ by definition over a horizontal surface. Therefore from Eq. (20) we can write $\overline{\nabla\cdot\mathbf{H}} = -\overline{\partial_z H} = -\overline{Q_{\rm rad}}$. Given the mean flux at the surface, $\overline{H}_{1/2}$, and $\overline{\partial_z H}_k$, it is thus possible to work out $\overline{H}_{k+1/2}$ at every model half-level ($Q_{\rm rad}$ is defined on the full model levels, k). $\overline{H}$ (mass-weighted with the thickness of the model layer) is shown in Fig. 8b (lower panel) and Fig. 10d. The vertical material heat flux profiles form three different clusters (apart from $T_{\rm NOH}$ whose flux is null by construction). The most vigorous vertical energy transport is associated with $T_{\rm NOT}$ and $T_{\rm NOVT}$ as expected, since again they are the by construction climates with no vertical temperature gradient and thus strong vertical mixing. $T_{\rm NOHT}$ and $T_{\rm NOHH}$ cluster together with $T_{\rm CLIM}$, as to define them we only rearranged temperature on horizontal levels leaving untouched the vertical structure. Their vertical fluxes have maximum value at the surface and decrease monotonically with height (beyond 400 hPa the fluxes go practically to zero). The MEP (MEP2) profile differs quite substantially from the FAMOUS one and from the first cluster. It is intermediate in terms of magnitude of $\overline{H}$ but with a lower surface value (~80 W m^{-2}. However it tends to increase with altitude and reaches a maximum around 700 hPa, after which it slowly decreases to zero. This difference can be partially understood if we look at the radiative heating rates (not shown): the MEP (MEP2) solution has its cooling region peaked mostly at 400–200 hPa, which is notably higher than in FAMOUS (800–400 hPa). In a steady state the radiative cooling has to be balanced by the convergence of the material heat fluxes. The material entropy production of the horizontally averaged vertical model is written as (Ozawa and Ohmura (1997); Pujol and Fort (2002)):

$$\dot{S}_{\rm ver} = \sum_k \overline{H}_{k+1/2}\left(\frac{1}{\overline{T}_{k+1}} - \frac{1}{\overline{T}_k}\right) \tag{21}$$

in which $\overline{T}_k$ is simply the mean surface temperature at level k. The contribution of each model layer to $\dot{S}_{\rm ver}$, i.e. $\dot{S}_{{\rm ver},k} = \overline{H}_{k+1/2}\dot{S}_{{\rm ver},k}$, is shown in Fig. 9a and b for the different temperature configurations. As it can be seen in Table 3, $\dot{S}_{\rm ver}$ is the term that really

ESDD
2, 393–434, 2011

makes the difference between the MEP state and all the others. Features to be pointed out are: (i) the first term $\dot{S}_{\mathrm{ver},1/2}$ is substantially greater than zero ($\sim 7\,\mathrm{mW\,m^{-2}\,K^{-1}}$) due to the outstanding surface-atmosphere discontinuity which is a feature of the MEP solution; (ii) contributions from the middle-upper atmosphere remain significant, as shown in Figs. 9a–b. In other words the MEP solution is "trying" to raise the surface temperature in order to reduce the entropy gain from insolation, and also "trying" to get the heat as high as it can in the atmosphere before radiating it to space, in order to increase the entropy loss. Together these tendencies increase the material entropy production as can be deduce from Eq. (15).

6 Varying temperature and τ simultaneously

Finally we consider simultaneous variations of the longwave transmissivity τ and the temperature field T, and assume $\epsilon = 1 - \tau$. Therefore under the constraint Eq. (16) we look for T and τ such that:

$$\frac{\delta \dot{S}_{\mathrm{mat}}}{\delta T}[T_{\mathrm{MEP}}, \tau_{\mathrm{MEP}}] = 0, \quad \frac{\delta \dot{S}_{\mathrm{mat}}}{\delta \tau}[T_{\mathrm{MEP}}, \tau_{\mathrm{MEP}}] = 0. \tag{22}$$

The way the variational problem is now formulated will inevitably lead to unphysical configurations, because, as already said in Sect. 3.1, the longwave optical properties depend, in a complicated way, on the atmospheric conditions. Consequently most of the states which will be accessed during the variational process will violate the local thermodynamic equilibrium, which is the cornerstone assumption of any non-equilibrium problem (DeGroot and Mazur, 1984). What we want to show here is that MEP leads to nonsense results when, despite the fulfilment of the energy balance, local thermodynamic equilibrium is severely violated.

Again a drastic reduction of the degrees of freedom is necessary for making the problem numerically tractable with IMSL_CONSTRAINED_NLP, as explained in Sect. 4.1. Here we reduce the degrees of freedom from $12 \times 37 \times 48$ (FAMOUS resolution) to

ESDD
2, 393–434, 2011

$12 \times 5 \times 1$, that is we keep unchanged the vertical resolution, take the zonal mean and take 5 latitudinal zones. A MEP solution (TAUTEMP) is obtained for a material entropy production within the range $[160, 180]\,\mathrm{mW\,m^{-2}\,K^{-1}}$. Unlike the MEP solution in Sect. 5, which is fairly well defined and insensitive to the initial guess provided to IMSL_CONSTRAINED_NLP, the MEP solutions found now seem to show a "weak" dependence on the initial guess, where by "weak" we mean here that different solutions differ for values of entropy production by 15 % but show the same qualitative characteristics. Unfortunately it has not been possible to obtain a numerical solution for a higher resolution (at least comparable with the ones in Sects. 4–5) in order to check the convergence of the solution. Although the rigour of our results might be questionable, we will take them as an indication of what kind of temperature and longwave transmissivity tend to increase the material entropy production.

Let us first note that τ_{MEP} tends to zero in the lower and middle atmosphere and sharply goes to unity in the uppermost atmosphere (Fig. 11a), which means that the atmosphere becomes completely opaque to the longwave radiation except in the upper atmosphere, thus shifting up the Earth's emission level (i.e. the level from which most of the TOA longwave radiation is emitted). The enhanced greenhouse effect due to the τ_{MEP} pattern is associated with a generally warmer climate as can be seen in Fig. 11b, 12 and 13. Mean heat vertical fluxes (Fig. 13, lower panel) are very intense and extend higher into the atmosphere up to about 200 hPa (corresponding to the longwave cooling levels) where they drop drastically. The meridional heat flux is enhanced too (Fig. 12), correspondingly to an increase in the meridional gradient of the surface temperature.

Figure 14 shows the contributions at each level to the material entropy production $\dot{S}_{\mathrm{ver}}$ defined in Eq. (21). The main differences for CLIM and MEP (MEP2) come from the upper atmosphere in which a lot of entropy production takes place in TAUTEMP, due to the vigorous mean vertical flux (Fig. 13). This is a consequence of the peculiar pattern of τ_{MEP} (Fig. 11a). Most of the radiative cooling takes place in the upper atmosphere where τ_{MEP} sharply goes from zero to one (the longwave radiation emitted underneath is completely absorbed and does not cool the atmosphere). This cooling has to be

ESDD
2, 393–434, 2011

balanced by the convergence of the material vertical fluxes. Therefore in TAUTEMP we have a heat flux between the surface and the higher atmosphere and thus through a temperature gradient (~80 K) much higher than normal (~30 K).

7 Conclusions

This paper provides insights on MEP application to a minimal box-model of climate. This minimal box-model of the climate must be able to represent both horizontal (meridional) and vertical heat fluxes and temperature gradients since these are the major characteristics of our climate system. By keeping insolation and optical properties of each atmospheric box fixed (i.e. the surface albedo, shortwave and longwave transmissivity), a MEP solution can be found with numerical values of temperatures and heat fluxes reasonably realistic given the simplicity of the model. This results extend the two-box analysis of Lorenz et al. (2001) and Kleidon (2009), by putting together the two basic box-models for horizontal and vertical motions only. The analysis of the "horizontal" $\dot{S}_{\mathrm{mer}}$ and "vertical" $\dot{S}_{\mathrm{ver}}$ component of the material entropy production shows that $\dot{S}_{\mathrm{mer}}$ is almost independent from H_1 and H_2. Since $\dot{S}_{\mathrm{mer}}$ is entirely due to atmospheric processes, this result seems consistent with the maximum power conjecture discussed in Kleidon (2010) in terms of a two-box model. Also, $\dot{S}_{\mathrm{ver}}$ is independent of M i.e. horizontal and vertical material entropy production are independent.

Further insight is obtained by considering a zonal-vertical model of climate analogous to the four-box model but with increased degrees of freedom. Radiative parameters (shortwave and longwave transmissivity) are derived from a GCM climatology. By using *ad hoc* temperature configurations we obtain an order-of-magnitude decomposition of the total material entropy production ($\approx 50\,\mathrm{mW\,m^{-2}\,K^{-1}}$) in its horizontal component $\dot{S}_{\mathrm{mer}} \approx 5\text{–}7\,\mathrm{mW\,m^{-2}\,K^{-1}}$ and its vertical component $\dot{S}_{\mathrm{ver}} \approx 40\,\mathrm{mW\,m^{-2}\,K^{-1}}$ i.e. vertical EP dominates.

A MEP solution is found either at $\dot{S}_{\mathrm{mat}} \approx 70\ \mathrm{mW\,m^{-2}\,K^{-1}}$ or $\dot{S}_{\mathrm{mat}} \approx 57\ \mathrm{mW\,m^{-2}\,K^{-1}}$ for two different longwave parametrisations. In both cases the MEP solutions show a

ESDD
2, 393–434, 2011

surprising realism as far as the surface temperature and transport of meridional heat are concerned but major discrepancies with FAMOUS climatology (assumed as representative of real climate, see Jones et al. (2005)) are found in the vertical organisation of the atmosphere. The MEP solution has an unrealistic surface-atmosphere temperature discontinuity (≈6 K), as also found in Pujol and Fort (2002), and to be more vertically mixed, consistently with the mean vertical structure of heat flux (Fig. 8b). The entropy surplus thus found in the MEP solution with respect to the FAMOUS one is shown to be due to these major vertical differences. We note that MEP does not give us a temperature field which is fully thermodynamically consistent with the FAMOUS distribution of longwave transmissivity. That implies, perhaps weakly, that the real world is not in an MEP state. This is made even more visible in a second experiment, in which also the longwave transmissivity is varied simultaneously with the temperature field. This leads to a completely unrealistic MEP solution ($\dot{S}_{\mathrm{mat}} \approx 160\,\mathrm{mW\,m^{-2}\,K^{-1}}$) characterised by a much warmer climate with very strong vertical heat fluxes and by an atmosphere completely opaque to longwave radiation which sharply becomes transparent in its upper polar regions. This last MEP solution is clearly more unrealistic than the MEP solution found in the case in which τ was kept fixed at its climatological values but it can be seen that these deviations from reality will indeed tend to increase the entropy production subject to fixed shortwave absorption.

This substantial difference in the two solutions found under two different model formulations rises important scientific issue about the importance of the boundary conditions and the model formulation for the success of MEP (see also Goody, 2007). It seems that if the proper physical "ingredients" are not included in a low complexity climate model (as in Sect. 6), the answer given by MEP is not realistic. In fact it is unrealistic to think of the longwave transmissivity as a variable independent from temperature, as in reality it strongly depends on water vapour concentration and thus temperature. Also, the large near-surface vertical temperature profile is not supportable in the real fluid atmosphere. Moreover we argue that the definition of the model has to be such that the set of steady states obtained under never violate the local thermodynamic equilibrium,

ESDD
2, 393–434, 2011

which should be considered not as a further physical ingredient but as a necessary condition to deal with non-equilibrium steady states. This seems to be a stricter re-definition of MEP formulation than what believed in Dewar (2009) or Dyke and Kleidon (2010), according to which MEP is an inference algorithm that passively translates physical assumptions into macroscopic predictions (as MaxEnt, Jaynes (1957)).

As discussed in Goody (2007) and shown, for example, in Pascale et al. (2011b), unconstrained and constrained MEP may give results and mechanisms which are radically different from each other. Further research is therefore needed in order to test the importance of the local thermodynamic equilibrium, external dynamical constraints (e.g. the Earth rotation speed) and of constrained problems in MEP, and their impact on predictions deriving from MEP.

Acknowledgements. SP acknowledge the financial support of the Reading International studentship and EU-ERC research grant NAMASTE. VL also acknowledges the NAMASTE grant. JG acknowledges support from the NCAS-Climate programme and the joint DECC and Defra Integrated Climate Programme, DECC/Defra (GA01101).

References

Caldeira, K.: The maximum entropy principle: a critical discussion, Clim. Change, 85, 267–269, 2007. 394

DeGroot, S. and Mazur, P.: Non-equilibrium thermodynamics, Dover, 1984. 410

Dewar, R. C.: Maximum entropy production and the fluctuation theorem, Journal of Physics A, 38, L371–L381, 2005. 395

Dewar, R. C.: Maximum entropy production as an inference algorithm that translates physical assumption into macroscopic predictions: don't shoot the messenger, Entropy, 11, 931–944, 2009. 396, 414

Dufresne, J., Fournier, R., Hourdin, C., and Hourdin, F.: Net exchange reformulation of radiative transfer in the CO_2 15 µm band on Mars, J. Atmos. Sci., 62, 3303–3319, 2005. 396

Dyke, J. and Kleidon, A.: The maximum entropy production principle: its theoretical foundations and applications to the earth system, Entropy, 12, 613–630, 2010. 396, 414

ESDD

2, 393–434, 2011

Edwards, J. and Slingo, A.: Studies with a flexible new radiation code. Part one: Choosing a configuration for a large-scale model, Q. J. Roy. Meteor. Soc., 122, 689–719, 1996. 401, 402
Fraedrich, K. and Lunkeit, F.: Diagnosing the entropy budget of a climate model, Tellus A, 60(5), 921–931, 2008. 395
Goody, R.: Sources and sinks of climate entropy, Q. J. Roy. Meteorol. Soc., 126, 1953–1970, 2000. 402
Goody, R.: Maximum entropy production in climate theory, J. Atmos. Sc., 64, 2735–2739, 2007. 394, 396, 413, 414
Gordon, C., Cooper, C., Senior, C., Banks, H., Gregory, J., Johns, T., Mitchell, J., and Wood, R. A.: The simulation of SST, sea ice extents and ocean heat transports in a version of the Hadley Centre coupled model without flux adjustments, Clim. Dynam., 16, 147–168, 2000. 400
Grassl, H. The climate at the maximum-entropy production by meridional atmospheric and oceanic heat fluxes, Q. J. Roy. Meteor. Soc., 107, 153–166, 1981. 395
Grinstein, G. and Linsker, R.: Comments on a derivation and application of the maximum entropy production principle, J. Phys A, 40, 9717–9720, 2007. 395
Herbert, C., Paillard, D., and Dubrulle, B.: Entropy production and multiple equilibria: the case of the ice-albedo feedback, Earth Syst. Dynam., 2, 13–23, doi:10.5194/esd-2-13-2011, 2011. 395
Herbert, C., Paillard, D., Kageyama, M., and Dubrulle, B.: Present and last glacial maximum climates as states of maximum entropy production, http://arxiv.org/abs/1101.3173, 2001. 395, 396
Ito, T. and Kleidon, A.: Non-equilibrium thermodynamics and the production of entropy, chapter 8, Entropy production of atmospheric heat transport, 93–106, Springer, 2005. 406
Jaynes, E.: Information theory and statistical mechanics. Phys. Rev., 106, 620–630, 1957. 414
Jones, C., Gregory, J., Thorpe, R., Cox, P., Murphy, J., Sexton, D., and Valdes, P.: Systematic optimisation and climate simulation of FAMOUS, a fast version of HadCM3, Clim. Dynam., 25, 189–204, 2005. 400, 413
Jupp, T. and Cox, P.: MEP and planetary climates: insights from a two-box climate model containing atmospheric dynamics, Philos. T. R. Soc. B, 365, 1355–1365, 2010. 395
Kleidon, A.: Beyond gaia: thermodynamic of life and earth system functioning, Climatic Change, 66, 271–319, 2004. 395
Kleidon, A.: Nonequilibrium thermodynamics and maximum entropy production in the earth

ESDD
2, 393–434, 2011

system, Naturwissenschaften, 96, 653–677, 2009. 395, 398, 399, 405, 406, 407, 412
Kleidon, A.: A basic introduction to the thermodynamics of the earth system far from equilibrium and maximum entropy production, Philos. T. R. Soc. B, 365, 1303–1315, 2010. 395, 412
Kleidon, A., Fraedrich, K., and T. Kunz F. Lunkeit, F.: The atmospheric circulation and the states of maximum entropy production, Geophys. Res. Lett., 30(23), 2223, doi:10.1029/2003GL018363, 363, 2003. 400
Kleidon, A., Fraedrich, K., Kirk, E., and Lunkeit, F.: Maximum entropy production and the strenght of boundary layer exchange in an atmospheric general circulation model, Geophys. Res. Lett., 33, L06706, doi:10.1029/2005GL025373, 373, 2006. 400
Kunz, T., Fraedrich, K., and Kirk, E.: Optimisation of simplified GCMs using circulation indices and maximum entropy production, Clim. Dynam., 30, 803–813, 2008. 400
Lorenz, R., Lunine, J., Withers, P., and McKay, C.: Titan,Mars and Earth: Entropy production by latitudinal heat transport, Geophys. Res. Lett., 28(3), 415–418, 2001. 395, 400, 412
Lucarini, V., Fraedrich, K., and Ragone, F.: Thermodynamical properties of planetary fluid envelopes, J. Atmos. Sci., in revision, 2010. 398
Murakami, S. and Kitoh, A.: Euler-Lagrange equation of the most simple 1-d climate model based on the maximum entropy production hypothesys, Q. J. Roy. Meteor. Soc., 131(608), 1529–1538, 2005. 400
Noda, A. and Tokioka, T.: Climates at minima of the entropy exchange rate, Journal of Meteorological Society of Japan, 61, 894–908, 1983. 395, 406
Ozawa, H. and Ohmura, A.: Thermodynamics of a global-mean state of the atmosphere: A state of maximum entropy increase, J. Climate, 10, 441–445, 1997. 399, 400, 405, 407, 409
Paltridge, G.: Thermodynamic dissipation and the global climate system, Q. J. Roy. Meteor. Soc., 107, 531–547, 1981. 395
Paltridge, G. W.: Global dynamics and climate-a system of minimum entropy exchange, Q. J. Roy. Meteor. Soc., 101, 475–484, 1975. 394, 395
Paltridge, G. W.: The steady state format of global climate, Q. J. Roy. Meteor. Soc., 104, 927–945, 1978, 395, 396, 406
Pascale, S., Gregory, J., Ambaum, M., and Tailleux, R.: Climate entropy budget of the HadCM3 atmosphere-ocean general circulation model and FAMOUS, its low-resolution version, Clim. Dynam., 36(5–6), 1189–1206, 2011a. 395, 396, 400, 402, 403
Pascale, S., Gregory, J., Ambaum, M., and Tailleux, R.: A parametric sensitivity study of entropy production and kinetic energy dissipation using the FAMOUS AOGCM, Clim. Dynam.,

ESDD
2, 393–434, 2011

doi:10.1007/s00382-011-0996-2, 2011b. 396, 414
Pope, V. D., Gallani, M. L., Rowntree, P. R., and Stratton, R. A.: The impact of new physical parametrizations in the Hadley Centre climate model – HadAM3, Clim. Dynam., 16, 123–146, 2000. 400
Pujol, T. and Fort, J.: States of maximum entropy production in a one-dimensional vertical model with convective adjustments, Tellus A, 54, 363–369, 2002. 399, 400, 405, 407, 408, 409, 413
Rodgers, C.: Minimum entropy exchange principle-reply, Q. J. Roy. Meteor. Soc., 102, 455–457, 1976. 400
Schulman, L. L.: A theoretical study of the efficiency of the general circulation, J. Atmos. Sci., 34, 559–580, 1977. 406
Smith, R. S., Gregory, J. M., and Osprey, A.: A description of the FAMOUS (version xdbua) climate model and control run, Geoscientific Model Development, 1, 147–185, 2008. 400
Spellucci, P.: An SQP method for general nonlinear programs using only equality constrained subproblems, Math. Prog., 82, 413–448, 1998. 406
Wang, B., Nakajima, T., and Shi, G.: Cloud and water vapor feedbacks in a vertical energy-balance model with maximum entropy production, J. Climate, 21(24), 6689–6698, 2008. 405

ESDD
2, 393–434, 2011

Table 1. Parameters used in the box-model shown in Fig. 1. The values have been obtained from a HadCM3 control run after defining a "tropical" box in the GCM with edges at 30° N–30° S and an "extra-tropical" box for the complementary polar caps. With this choice the areas of the two boxes are equal. τ_l has been worked out by using the approximation in Eq. (12) and defined for the box-model as the total transmissivity of the atmosphere, i.e. the product of τ_l at all atmospheric levels.

Quantity		Box 1	Box 2
Insolation ($W\,m^{-2}$)	I	302	180
LW transmissivity	τ_l	0.018	0.034
SW transmissivity	τ_s	0.70	0.62

ESDD
2, 393–434, 2011

Table 2. Values of the variables defining the minimal box-model in Fig. 1 obtained from the maximisation of $\dot{S}_{\mathrm{mat}}(M, H_1, H_2)$ and from a HadCM3 control run after defining a "tropical" and "extra-tropical" zone in the GCM with edges at 30° N–30° S. Values of the total and vertical material entropy productions are averaged over the two zones.

Quantity		MEP	HadCM3	Units
Vertical heat flux 1	H_1	113	138	$\mathrm{W\,m^{-2}}$
Vertical heat flux 2	H_2	55	64	$\mathrm{W\,m^{-2}}$
Meridional heat	M	34.5	39	$\mathrm{W\,m^{-2}}$
Atmospheric temperature 1	$T_{a,1}$	261.7	258	K
Atmospheric temperature 2	$T_{a,2}$	247.5	247	K
Surface temperature 1	$T_{g,1}$	282.2	298	K
Surface temperature 2	$T_{g,2}$	260.7	277	K
Material entropy production	$\dot{S}_{\mathrm{mat}}$	28.8	51	$\mathrm{mW\,m^{-2}\,K^{-1}}$
Horizontal entropy production	$\dot{S}_{\mathrm{mer}}$	7.5	–	$\mathrm{mW\,m^{-2}\,K^{-1}}$
Vertical entropy production	$\dot{S}_{\mathrm{ver}}$	21.2	–	$\mathrm{mW\,m^{-2}\,K^{-1}}$

ESDD
2, 393–434, 2011

Table 3. Entropy production summary for the seven temperature configurations. All entropy production in $\mathrm{mW\,m^{-2}\,K^{-1}}$.

climate	$\dot{S}_{\mathrm{mat}}$	$\dot{S}_{\mathrm{vert}}$	$\dot{S}_{\mathrm{mer}}$ (residual)
CLIM	47	40	7
MEP	70	62	8
NOHT	39	38	1
NOHH	41	41	0
NOVT	6	0	6
NOT	0	0	0
NOH	0	0	0

ESDD
2, 393–434, 2011

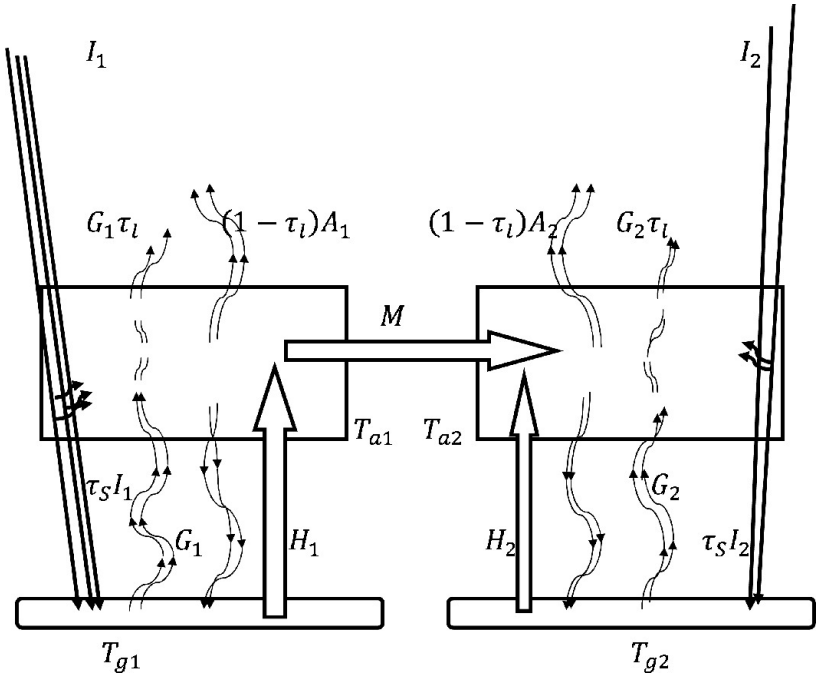

Fig. 1. Minimal model for representing the material entropy production of the climate system. The model consists of "tropical" and "high-latitude" surface-atmosphere components which exchange heat via the meridional transport M. The surface and the atmosphere interact through the fluxes H_1 and H_2 (latent and sensible heat).

ESDD
2, 393–434, 2011

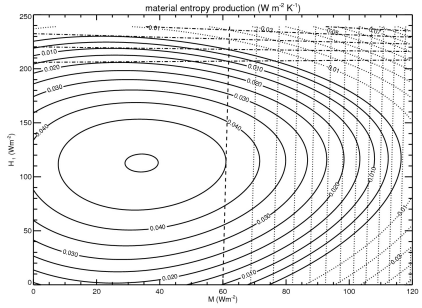

(a)

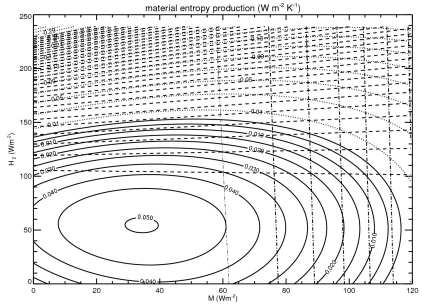

(b)

Fig. 2. **(a)** $\dot{S}_{\mathrm{mat}}$ in the (M,H_1) plane at $H_2 = H_{2,\mathrm{mep}}$ and **(b)** $\dot{S}_{\mathrm{mat}}$ in the (M,H_2) plane at $H_2 = H_{1,\mathrm{mep}}$. The dashed and dotted lines indicate the unphysical portion of the flux-space in which either $\dot{S}_{\mathrm{mer}}$ and $\dot{S}_{\mathrm{ver},1}$ ($\dot{S}_{\mathrm{ver},2}$ in **(b)**) are negative (compare with Figs. 3b–5b).

ESDD
2, 393–434, 2011

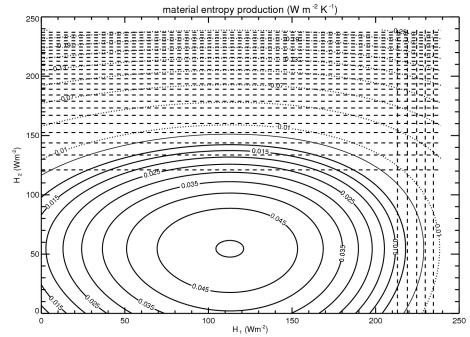

(a)

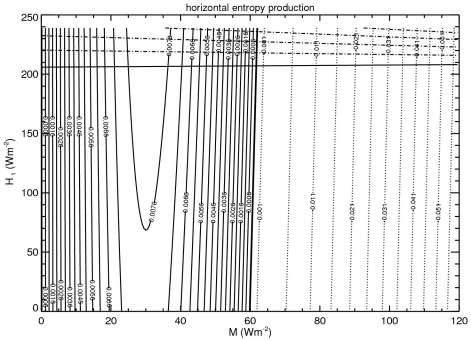

(b)

Fig. 3. **(a)** $\dot{S}_{\mathrm{mat}}$ in the (H_1, H_2) plane at $M = M_{\mathrm{mep}}$ and **(b)** $\dot{S}_{\mathrm{mer}}$ in (M, H_1) plane at $H_2 = H_{2,\mathrm{mep}}$. The dashed and dotted lines indicate the unphysical portion of the flux-space in which either $\dot{S}_{\mathrm{mer}}$ and $\dot{S}_{\mathrm{ver},2}$ are negative.

ESDD
2, 393–434, 2011

MEP solution for a climate model

S. Pascale et al.

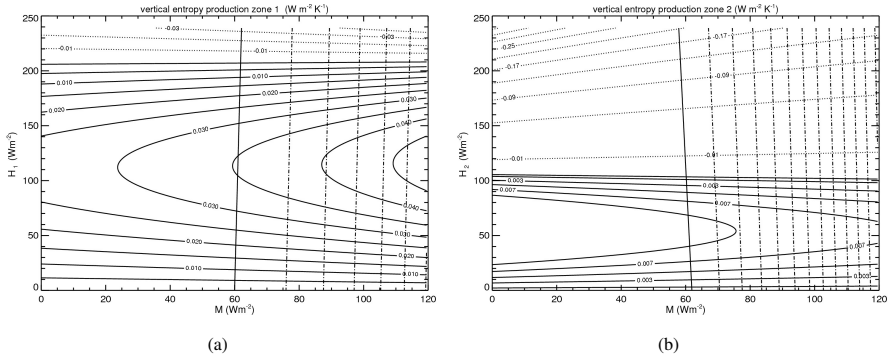

Fig. 4. (a) $\dot{S}_{\mathrm{ver},1}$ and **(b)** $\dot{S}_{\mathrm{ver},2}$. Dot-dashed lines are areas of negative $\dot{S}_{\mathrm{mer}}$.

ESDD
2, 393–434, 2011

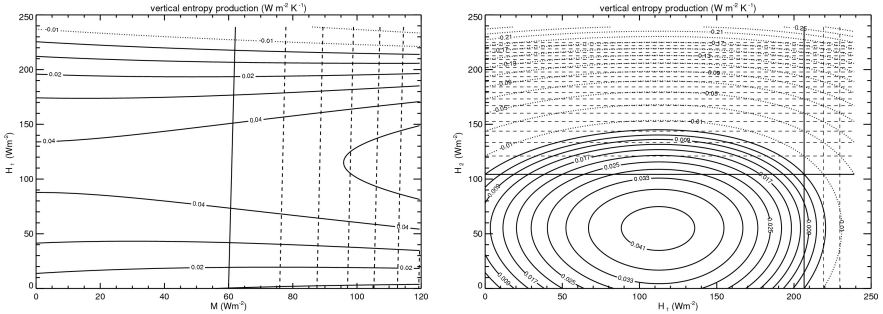

Fig. 5. **(a)** $\dot{S}_{\mathrm{ver}}$ in (M,H_1) plane at $H_2 = H_{2,\mathrm{mep}}$ (dashed lines denote the unphysical region of negative $\dot{S}_{\mathrm{mer}}$) and **(b)** $\dot{S}_{\mathrm{ver}}$ in (H_1,H_2) plane at $M = M_{\mathrm{mep}}$ (with areas of negative $\dot{S}_{\mathrm{ver},1}$ and $\dot{S}_{\mathrm{ver},2}$ overdotted).

ESDD
2, 393–434, 2011

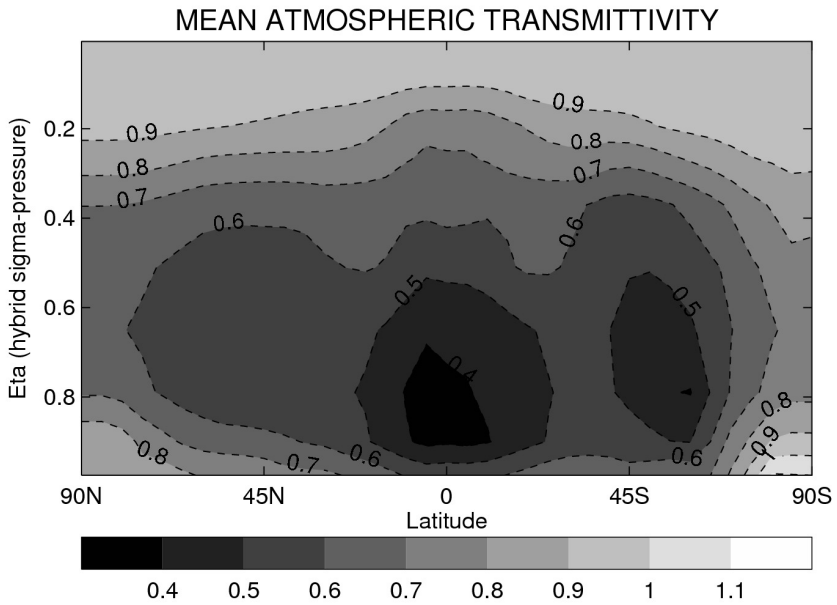

(a)

Fig. 6. Atmospheric transmissivity from a 30-year mean FAMOUS control run.

ESDD
2, 393–434, 2011

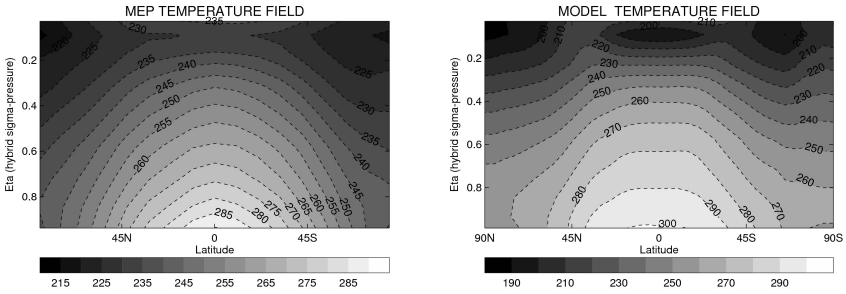

(a) MEP temperature field as obtained from the maximisation problem discussed in Section 5.

(b) FAMOUS temperature field. The values are obtained from a 30-year mean.

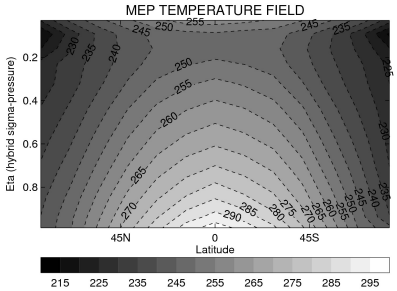

(c) MEP2 maximising atmospheric temperature

Fig. 7. (a) MEP temperature field as obtained from the maximisation problem discussed in Sect. 5. **(b)** FAMOUS temperature field. The values are obtained from a 30-year mean. **(c)** MEP2 maximising atmospheric temperature.

ESDD
2, 393–434, 2011

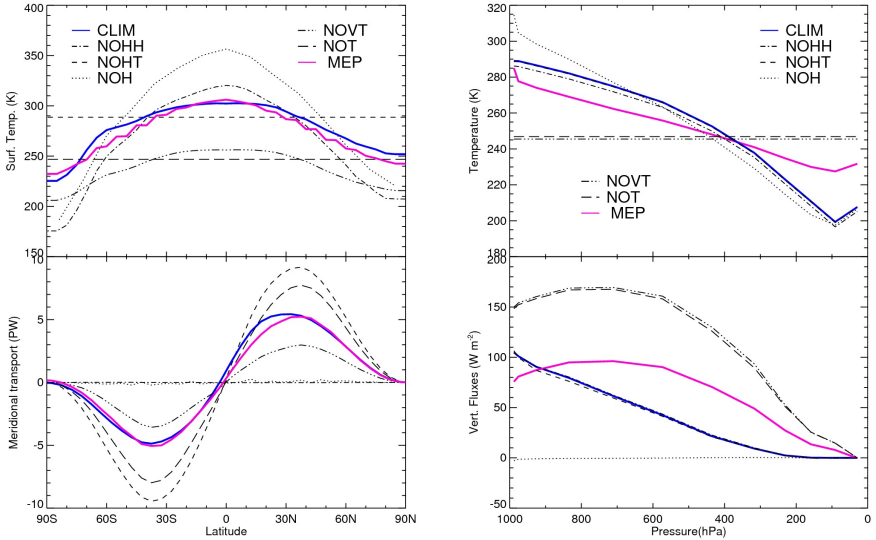

(a) (b)

Fig. 8. **(a)** Surface temperature (upper panel) and meridional heat transport (lower panel) coloured for the MEP solution and for the FAMOUS one (CLIM); **(b)** as in **(a)** but for the mean vertical profile and the mean vertical fluxes.

ESDD
2, 393–434, 2011

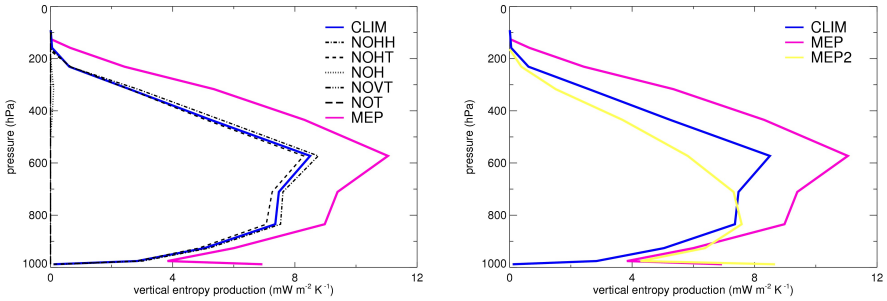

Fig. 9. (a) Contributions to $\dot{S}_{\mathrm{vert}}$ from each model level. **(b)** Comparison with MEP2.

ESDD
2, 393–434, 2011

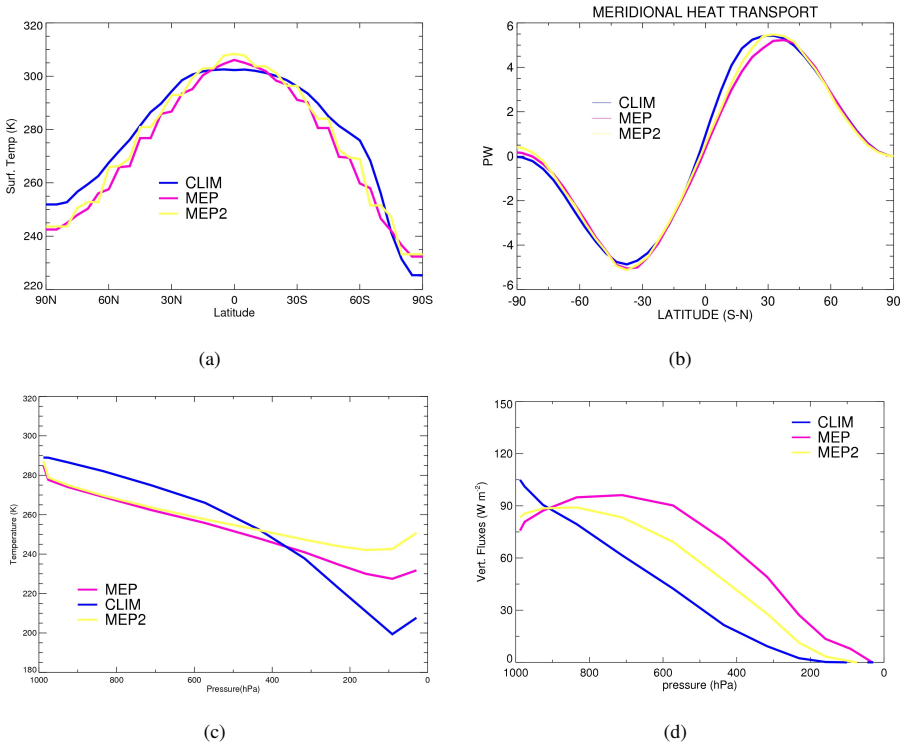

Fig. 10. Surface temperature **(a)**, meridional heat transport **(b)**, global mean temperature vertical profile **(c)** global mean vertical heat flux **(d)** for FAMOUS control run (CLIM), MEP and MEP2.

ESDD
2, 393–434, 2011

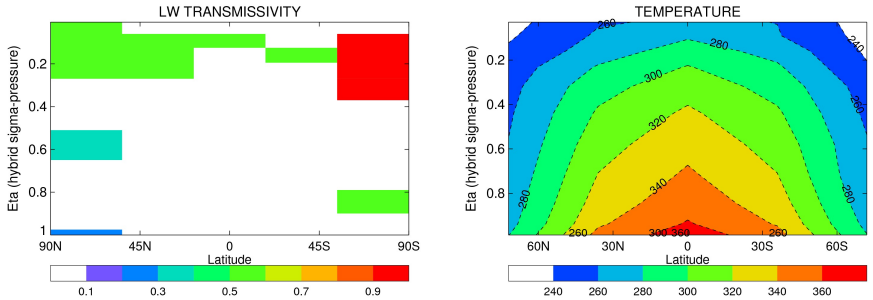

Fig. 11. LW transmissivity **(a)**, atmospheric temperature **(b)** for the first TAUTEMP solution ($\dot{S}_{\mathrm{mat}} \approx 160\,\mathrm{mW\,m^{-2}\,K^{-1}}$), CLIM and MEP.

ESDD
2, 393–434, 2011

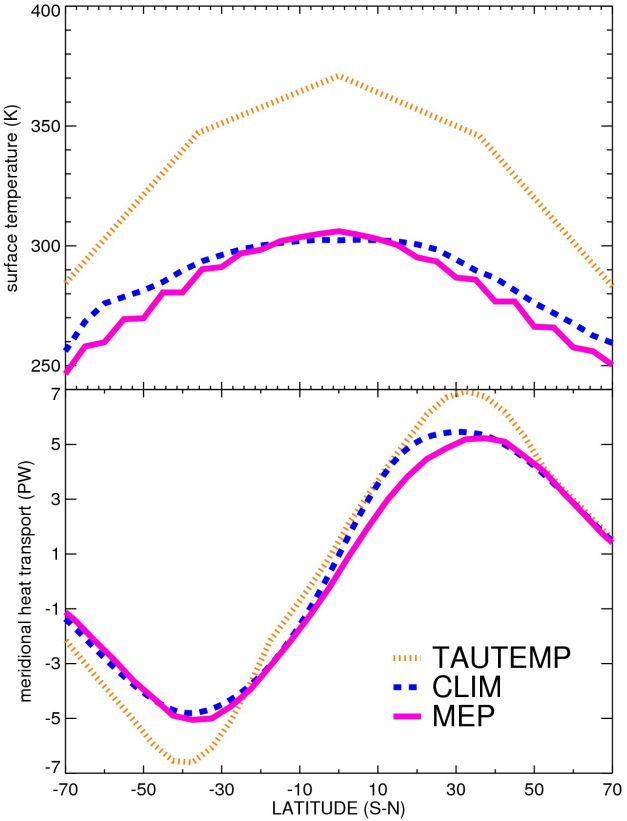

Fig. 12. **(a)** Surface temperature and **(b)** meridional heat transport for the TAUTEMP solution ($\dot{S}_{\mathrm{mat}} \approx 160\,\mathrm{mW\,m^{-2}\,K^{-1}}$), CLIM and MEP.

ESDD
2, 393–434, 2011

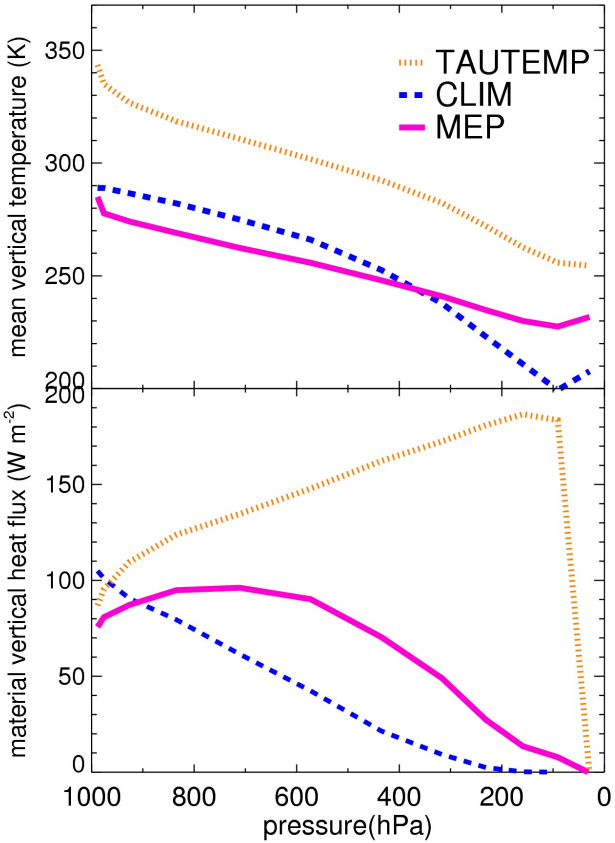

Fig. 13. **(a)** Mean vertical temperature profile and **(b)** mean vertical heat fluxes for the TAUTEMP solution ($\dot{S}_{\mathrm{mat}} \approx 160\,\mathrm{mW\,m^{-2}\,K^{-1}}$), CLIM and MEP.

ESDD
2, 393–434, 2011

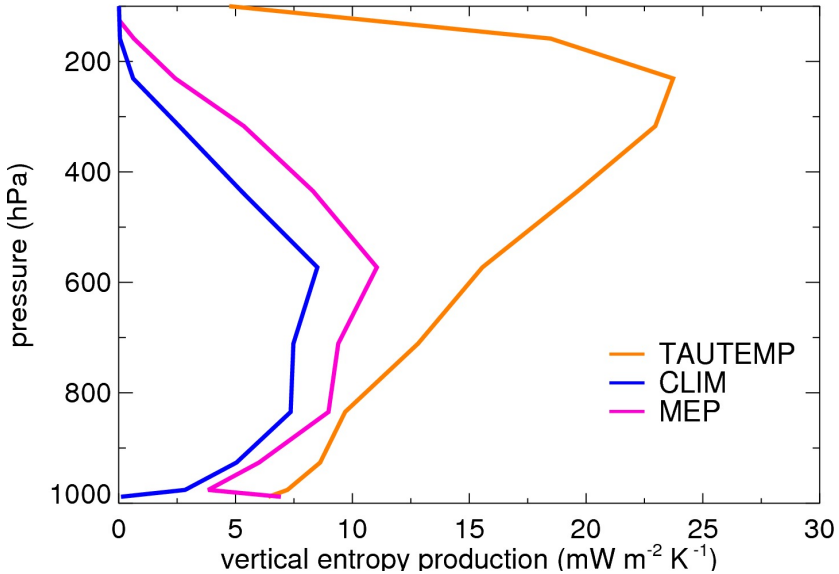

Fig. 14. Mean vertical entropy production contributions as in Eq. (21) for the TAUTEMP solution ($\dot{S}_{\mathrm{mat}} \approx 160\,\mathrm{mW\,m^{-2}\,K^{-1}}$), CLIM and MEP.

ESDD
2, 393–434, 2011